HHS Public Access

Author manuscript

Mech Dev. Author manuscript; available in PMC 2019 April 01.

Published in final edited form as:

Mech Dev. 2018 April ; 150: 21–27. doi:10.1016/j.mod.2018.02.003.

Genes and MicroRNAs Associated with Mouse Cleft Palate: A Systematic Review and Bioinformatics Analysis

Akiko Suzuki[1,2,#], **Nada Abdallah**[1,#], **Mona Gajera**[1,3], **Goo Jun**[3,4], **Peilin Jia**[5], **Zhongming Zhao**[3,4,5], and **Junichi Iwata**[1,2,4,*]

[1]Department of Diagnostic & Biomedical Sciences, School of Dentistry, The University of Texas Health Science Center at Houston, Houston, TX, USA

[2]Center for Craniofacial Research, The University of Texas Health Science Center at Houston, Houston, TX, USA

[3]Department of Epidemiology, Human Genetics & Environmental Sciences, School of Public Health, The University of Texas Health Science Center at Houston, Houston, TX, USA

[4]MD Anderson Cancer Center UTHealth Graduate School of Biomedical Sciences, Houston, TX, USA

[5]Center for Precision Health, School of Biomedical Informatics, The University of Texas Health Science Center at Houston, Houston, TX, USA

Abstract

Cleft palate (CP) is the most prevalent craniofacial deformity, with ethnic and geographic variation in prevalence in humans. Mice have been used as an animal model to study the cause(s) of CP by several approaches, including genetic and chemical-induced approaches. Mouse genetic approaches revealed that significant amounts of genes are involved in the CP pathology. The aim of this study was to identify common features of CP-associated genes and to explore the roles of microRNAs (miRNAs) as important post-transcriptional regulators that may be involved in the regulation of CP genes. To generate an accurate list of genes associated with CP, we first conducted systematic literature searches through main databases such as Medline, Embase, and PubMed, as well as other sources such as Scopus and Mouse Genome Informatics. We found that 195 mouse strains with single-gene mutations and 140 mouse strains with compound-gene mutations were reported to have CP. The CP genes were categorized by functions and pathways using the Kyoto Encyclopedia of Genes and Genomes and Gene Ontology annotations, highlighting the contribution of cellular metabolism to CP. A total of 18 miRNAs were involved in the regulation of multiple CP genes. Human genotype-phenotype analysis revealed that variants in five human homologous CP genes (*IRF6, FOXE1, VAX1, WNT9B*, and *GAD1*) significantly contributed to the human CP phenotype. Thus, our results suggest that cellular metabolism and

*Corresponding author, Junichi.Iwata@uth.tmc.edu.
#These authors equally contributed this study.

miRNAs play an important role in the regulation of genetic pathways and networks crucial for palatal formation.

Keywords

cleft palate; palate development; microRNA; gene mutation; systematic review; bioinformatics analysis

INTRODUTION

Cleft palate (CP) is among the most common human birth defects. It occurs approximately in one in 2,000 live births in the U.S., with ethnic and geographic variation in prevalence (Murray, 2002). CP can appear in both syndromic and nonsyndromic cases with various degrees of phenotypic severity (complete or partial CP [e.g. submucous CP, cleft soft palate]) (Lan et al., 2015). Individuals with CP require multidisciplinary care from birth through adulthood, including maxillofacial surgery, speech therapy, and dental treatments (Iwata et al., 2011). Genetic studies in humans and mice, as well as epidemiological studies, have identified a wide array of genetic and environmental risk factors for CP (Dixon et al., 2011; Leslie and Marazita, 2013). However, its etiology is not yet fully understood because of the complexity of genetic and environmental risk factors as well as gene–environment interactions. In addition, its complexity also derives from nonsyndromic cases, which can be sporadic or inherited as an autosomal dominant trait (Stanier and Moore, 2004).

The mouse as an animal model is well established and one of the most frequently used models to study the mechanism(s) of craniofacial development. This can be attributed to the facts that: 1) mouse palate development simulates that of humans', with a well-conserved molecular mechanism; 2) genetic background is homogenous; 3) environmental factors are under control; and 4) experimental time needed for their generation and analysis is measurable and short. Although mouse studies have identified significant amounts of CP-associated genes and signaling cascades, it remains unclear how these molecules and signaling pathways interact during palate formation.

Palatal development starts at the sixth week of gestation in humans and at embryonic day 11.5 (E11.5) in mice. The palatal shelves are composed of the mesenchyme derived from cranial neural crest cells (more than 95%) and mesodermal cells (less than 5%), covered with epithelial cells derived from the ectoderm (Iwata et al., 2012a). The palatal shelves first grow vertically along the tongue and then elevate into a horizontal position above the tongue, accompanied by growth of the mandible and descent of the tongue, around weeks 7–9 of gestation in humans and E13.5–E14.5 in mice. The elevated palatal shelves continuously grow horizontally toward each other and fuse by the 12^{th} week of gestation in humans and E16.5 in mice. The small anterior portion of the adult hard palate is known as the primary palate, which is formed from the frontonasal prominence, whereas the palatal shelves extending beyond the primary palate are called the secondary palate and form the majority of the hard (bony part) and soft (muscular part) palate that collectively separates the oral and nasal cavities. Disruption of any steps of palatogenesis, including growth, elevation, and fusion of the palatal shelves, results in CP (Ferguson, 1988; Iwata et al., 2011).

Accumulating evidence suggests that some of the genetic and epigenetic factors may target common functions (e.g. cell proliferation, differentiation) and pathways (e.g. growth factor signaling pathways) underlying CP. However, the regulatory networks of CP-associated genes and the contribution of epigenetic factors remain largely unknown.

Recent studies indicate that environmental factors modulate gene expression at the post-transcriptional level through the regulation of noncoding RNAs, including microRNAs (miRNAs) (Inui et al., 2010). The miRNA-gene regulatory mechanisms have been found to be critical in various diseases (Jiang et al., 2016; Sun et al., 2012). Several miRNAs (e.g. miRNA-140, miRNA-17-92 cluster, miRNA-200b, miRNA-133b) have been reported as CP-associated miRNAs in zebrafish and mouse models as well as humans (Schoen et al., 2017a).

To identify potential miRNAs that regulate CP-associated genes, we conducted a systematic review followed by bioinformatic analyses to identify common functional signatures and networks of CP-associated genes. In addition, we investigated the miRNA-gene interactions. This study will facilitate our understanding of the CP etiology and will help us extract molecular pathways crucial for palatal formation from the complexity of the CP etiology.

METHODS

Eligibility Criteria for the Systematic Review

The PRISMA (Preferred Reporting Items for Systematic reviews and Meta-Analyses) guideline and corresponding checklist were followed for this systematic review. Articles included in the systematic review met the following eligibility criteria: 1) described causative genes of mouse CP; 2) were published as original articles (not as review articles, editorials, or comments); 3) were published in English; 4) were published between the years 1980 and 2016; and 5) specified a CP type. Some articles were excluded from the systematic review because of one or more of the following reasons: 1) gene mutations were not described in the original articles; 2) CP was not described; 3) CP was caused by environmental factors; and 4) the articles failed to fit in any of the above criteria but did not have useful CP genes or related information.

Information Sources and Search

The online databases searched included Medline (Ovid), PubMed (National Library of Medicine), and EMBASE (Ovid). In addition, relevant citations were searched in Scopus (Elsevier) to retrieve any exceptional studies missed by the database searches. The bibliographies of highly pertinent articles were further examined to avoid any errors introduced with the systematic review. The Primary Excel Workbook designed for systematic reviews (http://libguides.sph.uth.tmc.edu/excel_SR_workbook) was used to track all search strategies and results, as described previously (Davlin and Vonville, 2012). The search was restricted to studies from 1980 to 2016 because mouse genetic studies have only advanced technologically in recent years.

Study Selection and Data Collection

RefWorks (Proquest) was utilized to store all the citations found through the search process. Titles and abstracts of papers found in the database search were screened using the Primary Excel Workbook, as described previously (Sangani et al., 2015). Data related to both screening and reviewing of the full text of articles not excluded were documented in the Primary Excel Workbook. A codebook including citation information, study-level information (characteristics and results), and quality level information was developed for data extraction from eligible articles.

Gene Set Enrichment Analysis

Gene set enrichment analysis was conducted using the WebGestalt tool (http://bioinfo.vanderbilt.edu/webgestalt) (Zhang et al., 2005). The Kyoto Encyclopedia of Genes and Genomes (KEGG) database (http://www.genome.jp/kegg) was used for canonical pathway enrichment analysis. Furthermore, the Gene Ontology (GO) database resource (http://www.geneontology.org) was used to identify functional categories of genes that were significantly enriched with CP-associated genes. Significantly enriched functional categories (pathways) were filtered to have a false discovery rate (FDR)-adjusted p-value <0.05 and at least four CP-associated genes. Here, p-value was calculated using the hypergeometric test. A hierarchical level 4 was used as the cut-off in order to avoid GO terms that were too general.

MicroRNA-Target Gene Analysis

The miRNA-gene relationships were verified with information from miRTarbase, the experimentally validated miRNA-gene interaction database, and three databases (miRanda, PITA, and TargetScan) of predicted miRNA-gene interactions (Chou et al., 2016; John et al., 2004; Kertesz et al., 2007; Lewis et al., 2005). Fisher's exact test was used to identify statistically significant miRNAs targeting multiple CP genes. The Benjamini Hochberg method was used for multiple test correction (Benjamini and Hochberg, 1995). FDR values were applied for all statistical analyses.

Identification of Human Association Signals of Mouse CP Genes

Genotype-phenotype association analysis was conducted using dbGaP resources available at the Center for Craniofacial and Dental Genetics (CCDG) (dbGaP accession phs000774.v1.p1), including 11,925 individuals, mostly from trios. Cases in this dataset include cleft lip (CL), CP, and CL and palate (CL/P) cases. All cases were nonsyndromic. We used CP with and without CL as cases and no CP/CL as controls. Whole-genome genotyping data from Illumina Infinium HumanCore BeadChips, including HumanCore v1 with added exome and custom contents by the CCDG consortium, were analyzed using PLINK (version 1.90b) for the association between the human CP phenotype and all directly genotyped variants of mouse CP genes listed through the systematic review. The genotype data contain the most common and rare variants for candidate genes of CP and CL genotypes. We performed single-variant association analyses for all single nucleotide polymorphisms (SNPs) existing within the mouse CP genes from the systematic review. We included all SNPs with more than 1% minor allele frequency. A transmission disequilibrium

test (TDT) of human genome-wide association studies (GWAS) for CP with or without CL phenotypes, which is a test for statistical imbalances between transmitted and non-transmitted alleles in parent-child trios, was applied for maximizing the analytical power for trios as well as for minimizing artifacts from population stratification (Spielman et al., 1993). A significant association between a SNP and CP phenotype means that there are children with the SNP who show higher prevalence of CP phenotypes than those who do not carry the SNP. We used two different multiple-testing thresholds for statistical significance: the Bonferroni threshold that accounts for the number of genes included in the testing and the nominal genome-wide significance threshold (5×10^{-8}). The Bonferroni level assumes that SNPs in the same gene are highly correlated with each other so it uses number of genes instead of number of SNPs for the multiple testing number. The widely-accepted genome-wide significance threshold was obtained from the effective number of genome-wide tests identified from the international HapMap project (International HapMap, 2003).

RESULTS

Literature and Database Search

A total of 4,577 articles were identified in the systematic review from year 1980 through 2016. After eliminating 2,528 duplicates from the list, the remaining 2,049 articles were further screened, using titles and abstracts, independently by the two screeners; 1,119 papers were excluded based on the reasons for exclusion. A total of 930 papers were further assessed for eligibility through full-text review; 360 studies met all inclusion criteria, and 570 articles were excluded based on the exclusion criteria during full-text manual review. As a result, we identified 360 studies eligible for further analysis in our systematic review (Figure 1). From these 360 studies, we identified 143 genes as mouse CP-associated genes.

Overview of the CP Studies

To date, the collective information for mouse phenotypes is stored in the Mouse Genome Informatics (MGI) database for search. We attempted to validate the information in the list of CP-associated genes from the systematic review with the MGI information. Through an MGI database search, a total of 616 genes or alleles were identified as CP-associated genes or alleles. Among those genes or alleles, only 166 genes (26.9%) were validated with full-text review. The remaining 450 genes or alleles (73.1%) listed in the MGI database were not validated through full-text review and were excluded from the CP-associated gene list. As a result from the systematic review and MGI database search, a total 195 genes were identified as CP-associated genes by either systematic review or MGI database-full text review search (see Table 1 in Suzuki et al., submitted). Among these 195 CP-associated genes, 58% (114 out of 195 genes) were common in the systematic review and MGI database search. There were 29 genes (15%, 29 out of 195 genes) and 52 genes (27%, 52 out of 195 genes) uniquely identified through the systematic review and MGI search, respectively (Figure 2).

We found that the CP phenotype has been reported in 301 mutant mice: CP caused by 195 single-gene mutations (see Table 1 in Suzuki et al., submitted), 27 spontaneous (unknown) mutations/deletions (see Table 2 in Suzuki et al., submitted), 9 chemical-induced CP (see Table 3 in Suzuki et al., submitted), and 70 compound mutations (see Table 4 in Suzuki et

al., submitted). The CP phenotype in mice with single-gene mutations was mostly the isolated, complete secondary CP (87.2%, 170 among 195 CP mouse lines); 25 out of 195 (12.8 %) CP mouse lines were partial CP, including anterior CP (11 lines: *Fgfr2, Gsc, Ihh, Lims1, Shox2, Sox11, Tbx1, Tbx3, Tgfb3, Tgfbr1*, and *Tgfbr2*), posterior CP (9 lines: *Bnc2, Foxf2, Hic1, Mef2c, Pax3, Sim2, Tgfbr1, Tgfbr2*, and *Tshz1*), and submucous CP (16 lines: *Acvr1, Apaf1, Arid5b, Csrnp1, Eya4, Krt5, Schip1, Sgpl1, Smad4, Tbx22, Tgfb3, Tgfbr1, Tgfbr2, Tiparp, Zfp640*, and *Zfp950*) (Table 1).

Gene Set Enrichment Analysis of Mouse CP Genes

For bioinformatics analyses, we excluded phenotypic markers and genes with unknown genomic location. For example, a phenotypic marker Sme for “Small ear” was excluded from the gene set enrichment analyses. In addition, spliced isoforms such as *Fgfr2b* and *Fgfr2c* were incompatible with further analyses. Pairs of genes in compound mutant mice (140 genes in 70 mouse lines) were incorporated into further analyses. In total, 255 protein-coding genes (see Tables 1 and 4 in Suzuki et al., submitted; overlapped genes were excluded) were subjected to gene set enrichment analysis for further analyses.

To identify molecular pathways crucial for palate formation, we conducted bioinformatics analyses of genes whose mutations accounted for CP in mice using functional annotations. The KEGG database has been established by collecting information from the literature and organizing it in a pathway map, ontology, and membership (Kanehisa, 2002). The KEGG represents one of the best-annotated canonical pathway databases. To analyze the biological functions of CP-associated genes, we performed category enrichment analysis for a variety of functional relations using the KEGG. Among the KEGG pathways, 46 were statistically enriched with CP-associated genes (see Table 5 in Suzuki et al., submitted). Within a category of molecular signaling pathways, 13 specific pathways were significantly enriched: signaling pathways of mitogen-activated protein kinase (MAPK) (19 CP genes), transforming growth factor beta (TGFβ) (14 CP genes), Wnt (8 CP genes), neurotrophin (7 CP genes), ErbB (6 CP genes), Hedgehog (5 CP genes), T-cell receptor (6 CP genes), B-cell receptor (5 CP genes), insulin (5 CP genes), gonadotropin-releasing hormone (GnRH) (5 CP genes), chemokine (6 CP genes), JAK-STAT (5 CP genes), and calcium (4 CP genes). This result is consistent with the fact that cell signaling pathways mediated by growth factors and morphogens play a critical role in palate development. Six KEGG pathways were enriched in a category of intercellular and cell surface structures: focal adhesion (16 CP genes), regulation of actin cytoskeleton (14 CP genes), adherens junction (10 CP genes), extracellular matrix (ECM)-receptor interaction (6 CP genes), gap junction (5 CP genes), cell adhesion molecules (4 CP genes), and cytokine-cytokine receptor interaction (13 CP genes). This suggests that the processes of cell adhesion/cell-cell contact are important for palatal development. Interestingly, the KEGG pathway analysis also highlighted the contribution of specific cell lineages, osteoclasts, and cranial nerves to CP: osteoclast differentiation (8 CP genes), and axon guidance (8 CP genes). These cell types have not been well considered as a cause of CP, but our results suggest investigating these cell lineages more carefully in palatogenesis and other developmental processes.

The CP-associated genes may be involved in other pathological conditions and may constitute a potential risk of future diseases. The KEGG analysis highlighted 21 pathways related to a variety of pathogeneses. Eleven of these enriched KEGG pathways reflected genes studied in cancers [pathway in cancer (28 CP genes), chronic myeloid leukemia (11 CP genes), prostate cancer (10 CP genes), renal cell cancer (10 CP genes), pancreatic cancer (9 CP genes), melanoma (9 CP genes), colorectal cancer (8 CP genes), endometrial cancer (6 CP genes), basal cell cancer (6 CP genes), glioma (5 CP genes) and small cell lung cancer (4 CP genes)]. Among them, molecules related to fibroblast growth factor (FGF), Hedgehog, and TGFβ signaling cascades were redundantly included in these cancer pathways because these signaling pathways accelerate the progression of cancers. Population-based studies suggest that individuals with CL with or without CP have a higher risk of cancer in the breast, brain, and lung later in life (Bille et al., 2005; Botto et al., 2013). Other three pathways indicated the involvement of CP-associated genes in cardiac diseases: hypertrophic cardiomyopathy (6 CP genes), dilated cardiomyopathy (6 CP genes), and arrhythmogenic right ventricular cardiomyopathy (4 CP genes). Because cardiac disorders are often reported in syndromic CP cases, the similar cellular and molecular mechanism may contribute to both craniofacial and cardiac development (Seto-Salvia and Stanier, 2014).

The KEGG pathway analysis also highlighted metabolic pathways (10 CP genes): *Papss2* in sulfur metabolism; *Sc5d, Tm7sf2, Dhcr7* in cholesterol biosynthesis; *Gad2* in butanoate metabolism, alanine, aspartate, and glutamate metabolism, beta-alanine metabolism, gamma-aminobutyrate (GABA) shunt, and taurine and hypotaurine metabolism; *Inpp5e* in inositol phosphate metabolism; *Glce* in lipid metabolism; *Piga* in glycosylphosphatidylinositol (GPI)-anchor biosynthesis; *Sgpl1* in sphingosine degradation; *Cdo1* in cysteine and methionine metabolism, and taurine and hypotaurine metabolism. Although increasing lines of evidence indicate that cellular metabolic aberrations increase the risk of CP (Khera, 1987; Suzuki et al., 2016), it remains largely unclear how metabolic aberrations cause CP.

Functional Categories of Mouse CP-Associated Genes

The GO is a comprehensive ontology database for annotation of gene features through numerous hierarchical terms into three main domains: Biological Process (BP), Molecular Function (MF), and Cellular Component (CC). The GO terms in BP and MF are especially useful for the interpretation of genes of interest (Lomax, 2005). To identify functional categories of CP-associated genes, we analyzed CP-associated genes using the GO database. As shown in the KEGG results, the most specific enriched terms among GO BP indicated a very strong association with metabolism: cellular macromolecule metabolic process (133 genes), regulation of cellular metabolic process (117 genes), regulation of primary metabolic process (117 genes), and regulation of macromolecule biosynthetic process (100 genes) (see Table 6 in Suzuki et al., submitted). Together with the KEGG pathway results, these results indicate that cellular metabolism plays an important role in palate development.

Among GO MF terms, we observed enrichment of several terms involving molecular binding and protein-interaction activities [ion binding (69 CP genes), identical protein binding (25 CP genes), protein domain specific binding (23 CP genes), regulatory region

nucleic acid binding (22 CP genes), chromatin binding (22 CP genes), transcription factor binding (17 CP genes), protein complex binding (17 CP genes), transcription regulatory region sequence-specific DNA binding (13 CP genes), glycosaminoglycan binding (10 CP genes), growth factor binding (11 CP genes), and SMAD (a family of signal transducers and transcriptional modulators that mediate TGFβ superfamily signaling) binding (11 CP genes)] (see Table 7 in Suzuki et al., submitted). These results are well matched with the fact that molecular complex formation and its DNA binding activated by growth and morphological factors play a crucial role in palate development.

Among GO CC terms, the CP genes were enriched in the cytoplasm (100 CP genes), plasma membrane part (26 CP genes), transcription factor complex in the nuclei (23 CP genes), and cell surface (16 CP genes) (see Table 8 in Suzuki et al., submitted). Some enriched terms were specifically related to a neuronal lineage: dendrite (12 CP genes), neuronal cell body (12 CP genes), and axon (11 CP genes), corresponding to the significant enrichment of cranial nerve in the KEGG analysis. Although the contribution of neurogenesis to palatogenesis remains unclear, these results suggest that innervation of cranial nerves may play an important role in palate development.

Genotype-Phenotype Association Analysis

To evaluate whether any of the SNPs in CP candidate genes reported in mouse CP are associated with the human CP phenotype, we conducted genotype-phenotype association analysis using CP GWAS data generated by CCDG and available from dbGaP (dbGaP accession phs000774.v1.p1), including 11,925 individuals, mostly from trios (see Methods). We applied the TDT to identify statistical imbalances between transmitted and non-transmitted alleles in parent-child trios of CP with or without a CL phenotype. By using CP with or without CL as case or control phenotype respectively, we identified 2,346 cases and 9,380 controls. We investigated whether the SNPs mapped to the CP candidate genes were associated with human CP phenotypes. We analyzed all directly genotyped (i.e. not imputed) variants within CP-associated genes. A total of 4,827 variants from 195 CP-associated genes were examined in the association analysis. Because most SNPs in the same gene had strong linkage disequilibrium, we set our candidate-wise significance threshold at 2.79×10^{-4} by using the Bonferroni level with the number of genes tested (0.05/179). We identified 10 SNPs from three genes (*IRF6, PDGFC*, and *VAX1*) with *p*-values $<2.79 \times 10^{-4}$ (Table 3). The top association signals were from *IRF6* (interferon regulatory factor 6), which also showed nominal genome-wide significance in the GWAS dataset (*p*-value $<5 \times 10^{-8}$). *PDGFC* (platelet-derived growth factor C) and *VAX1* (ventral anterior homeobox 1) did not reach the genome-wide significance threshold, but reached candidate gene-wise Bonferroni significance level (*p*-value $<2.79 \times 10^{-4}$).

Potential Regulatory Roles of miRNAs in CP

To explore the degree to which miRNAs regulate the expression of CP genes, we conducted enrichment analysis of known miRNA families and their targets (Table 4). With a FDR-adjusted *p*-value <0.001, our list of CP genes was significantly enriched with the targets of 18 miRNAs: mmu-miR-200a-3p (miR-8 family; 36 CP genes), mmu-miR-21a-5p (miR-21 family; 19 CP genes), mmu-miR-25-3p (miR-25 family; 28 CP genes), mmu-miR-92a-3p

(miR-25 family; 28 CP genes), mmu-miR-27a-3p (miR-27 family; 42 CP genes), mmu-miR-27b-3p (miR-27 family; 41 CP genes), mmu-miR-29b-3p (miR-29 family; 32 CP genes), mmu-miR-30a-5p (miR-30 family; 43 CP genes), mmu-miR-124-3p (miR-124 family; 55 CP genes), mmu-miR-377-3p (miR-154 family; 31 CP genes), mmu-miR-381-3p (miR-154 family; 39 CP genes), mmu-miR-185-5p (miR-185 family; 21 CP genes), mmu-miR-203-3p (miR-203 family; 39 CP genes), mmu-miR-320-3p (miR-320 family; 30 CP genes), mmu-miR-543-3p (miR-329 family; 28 CP genes), mmu-miR-590-5p (miR-590 family; 14 CP genes), and mmu-miR-882 (unknown family; 17 CP genes). These miRNAs regulate multiple CP genes, including several well-known early developmental genes such as *Msx2, Sox11*, and *Tgfbr1* (aka *Alk5*).

DISCUSSION

Human genetic variation differs according to ethnicity, population of origin, and gender, among others. Mouse genetic approaches have contributed to the understanding of the genetic control of palatogenesis [27]. A systematic review of the genes involved in complex disease or traits, followed by extensive bioinformatics and statistical analyses of the candidate genes, will not only be informative in the current status of the disease studies, but will also identify promising candidate genes and their regulation mechanisms for future validation (Sun et al., 2008; Wang et al., 2013b). In the present study, our systematic review identified 292 mouse lines (195 single-gene + 27 spontaneous + 70 compound mutations) with CP. The subsequent bioinformatics analyses of these CP genes provided genetic networks and functions that are likely crucial for palate development and that may help elucidate their roles in the etiology of CP. Genes involved in CP were enriched in signal transduction, transcriptional regulation, post-transcriptional regulation, and metabolism. Molecular mechanisms involved in post-transcriptional regulation and metabolism processes are not fully understood yet. Notably, the KEGG pathway analysis indicated that eight CP genes are involved in axon guidance; this was further supported by the GO cellular component analysis. In addition, the KEGG pathway analysis identified the enrichment of neurotrophin signaling pathway, which is involved in the differentiation and survival of neural cells. These results highlight a potential role of innervation of the maxillary nerve into the palatal shelves in palatogenesis that is currently unknown.

Environmental factors including maternal age, smoking, alcohol consumption, obesity, and micronutrient deficiencies are known or strongly suspected risk factors of CP. Recent studies indicate that epigenetic regulation by these environmental factors plays a crucial role in embryogenesis (Gou et al., 2015). Although most mouse lines with a single gene mutation or deletion exhibit CP by homozygous mutations, heterozygous mutations in the *Chrd, Col2a1, Fgfr2, Flna, Kat6a, Meox2, Mn1, Ofd1, Pds5a, Prdm16, Sox9, Sumo1, Tcof1*, and *Twist1* genes also resulted in CP. By contrast, human genetic studies show heterozygous gene mutations in human CP cases. The phenotypic differences in heterozygous vs homozygous mutations between humans and mice may be caused by the following two major reasons. First, multiple heterozygous gene mutations (combinations of various gene mutations) may be involved in human CP cases that were not studied by GWAS. In mouse models, several double heterozygous mutant mice exhibit CP although the single-gene heterozygous mutation fails to cause CP. In addition, compound mutant mice exhibit CP (and additional

craniofacial deformities in some mouse models) with different degrees of severity compared with mice with the single-gene mutation (Gritli-Linde, 2012; Iwata et al., 2013; Iwata et al., 2012b). Second, there are interactions between genetic and environmental factors in human cases. In humans, the exposure to some chemicals and intake of some foods may alter gene expression post-transcriptionally through epigenetic mechanisms, including miRNA regulation (Seelan et al., 2012; Wang et al., 2013a). In this study, we found that 18 miRNAs might regulate the expression of multiple CP genes. Importantly, except for mmu-miR-27b-3p (Wang et al., 2017) and mmu-miR-92a-3p (Schoen et al., 2017b), none of the remaining miRNAs have been reported in CP yet. Therefore, we expect possible new roles for these miRNAs in palatogenesis through future experimental work.

The principles learned from this study promise to be fertile ground for future molecular studies of craniofacial development, and will provide the basis for genetic tests and proper nutrient intake. Thus, the results from this study will have a significant impact on not only our knowledge of palatal morphogenesis, but also on the development of clinical approaches for diagnosis and prevention of CP.

Although our systematic review summarizes current CP-associated genes, it has some limitations. For example, some CP-associated genes found only in syndromes may be secondary to other defects. In addition, the current genetic signature of CP or other complex genetic diseases may be due to the bias of the type of genes that have been studied. The generation and characterization of mouse lines displaying CP are increasing. Mouse genetic and epigenetic approaches will thus provide us with a more detailed and accurate view of how genetic changes cause CP. In summary, this study will contribute to a better understanding of the molecular mechanisms (e.g. miRNA-gene pathways and networks) of CP and to future clinical interventions to prevent and diagnose CP.

Acknowledgments

We thank Mrs. Helena VonVille for her valuable assistance in the systematic review and Dr. Guangchun Han for assistance in the miRNA analysis. This study was supported by a grant from the National Institute of Dental and Craniofacial Research, NIH (DE024759, DE026208, DE026767, and DE026509 to J.I.), and a faculty start-up fund from the UT Houston School of Dentistry to J.I.

References

Benjamini Y, Hochberg Y. Controlling the false discovery rate: a practical and powerful approach to multiple testing. Journal of the royal statistical society Series B (Methodological). 1995:289–300.

Bille C, Winther JF, Bautz A, Murray JC, Olsen J, Christensen K. Cancer risk in persons with oral cleft--a population-based study of 8,093 cases. Am J Epidemiol. 2005; 161:1047–55. [PubMed: 15901625]

Botto LD, Flood T, Little J, Fluchel MN, Krikov S, Feldkamp ML, Wu Y, Goedken R, Puzhankara S, Romitti PA. Cancer risk in children and adolescents with birth defects: a population-based cohort study. PLoS One. 2013; 8:e69077. [PubMed: 23874873]

Chai Y, Jiang X, Ito Y, Bringas P Jr, Han J, Rowitch DH, Soriano P, McMahon AP, Sucov HM. Fate of the mammalian cranial neural crest during tooth and mandibular morphogenesis. Development. 2000; 127:1671–9. [PubMed: 10725243]

Chou CH, Chang NW, Shrestha S, Hsu SD, Lin YL, Lee WH, Yang CD, Hong HC, Wei TY, Tu SJ, Tsai TR, Ho SY, Jian TY, Wu HY, Chen PR, Lin NC, Huang HT, Yang TL, Pai CY, Tai CS, Chen WL, Huang CY, Liu CC, Weng SL, Liao KW, Hsu WL, Huang HD. miRTarBase 2016: updates to

the experimentally validated miRNA-target interactions database. Nucleic Acids Res. 2016; 44:D239–47. [PubMed: 26590260]

Davlin SL, Vonville HM. Canine rabies vaccination and domestic dog population characteristics in the developing world: a systematic review. Vaccine. 2012; 30:3492–502. [PubMed: 22480924]

Dixon MJ, Marazita ML, Beaty TH, Murray JC. Cleft lip and palate: understanding genetic and environmental influences. Nat Rev Genet. 2011; 12:167–78. [PubMed: 21331089]

Ferguson MW. Palate development. Development. 1988; 103(Suppl):41–60. [PubMed: 3074914]

Gou Y, Zhang T, Xu J. Transcription Factors in Craniofacial Development: From Receptor Signaling to Transcriptional and Epigenetic Regulation. Curr Top Dev Biol. 2015; 115:377–410. [PubMed: 26589933]

Gritli-Linde A. The mouse as a developmental model for cleft lip and palate research. Front Oral Biol. 2012; 16:32–51. [PubMed: 22759668]

International HapMap, C. The International HapMap Project. Nature. 2003; 426:789–96. [PubMed: 14685227]

Inui M, Martello G, Piccolo S. MicroRNA control of signal transduction. Nat Rev Mol Cell Biol. 2010; 11:252–63. [PubMed: 20216554]

Iwata J, Hacia JG, Suzuki A, Sanchez-Lara PA, Urata M, Chai Y. Modulation of noncanonical TGF-beta signaling prevents cleft palate in Tgfbr2 mutant mice. J Clin Invest. 2012a; 122:873–85. [PubMed: 22326956]

Iwata J, Parada C, Chai Y. The mechanism of TGF-beta signaling during palate development. Oral Dis. 2011; 17:733–44. [PubMed: 21395922]

Iwata J, Suzuki A, Pelikan RC, Ho TV, Sanchez-Lara PA, Urata M, Dixon MJ, Chai Y. Smad4-Irf6 genetic interaction and TGFbeta-mediated IRF6 signaling cascade are crucial for palatal fusion in mice. Development. 2013; 140:1220–30. [PubMed: 23406900]

Iwata J, Tung L, Urata M, Hacia JG, Pelikan R, Suzuki A, Ramenzoni L, Chaudhry O, Parada C, Sanchez-Lara PA, Chai Y. Fibroblast growth factor 9 (FGF9)-pituitary homeobox 2 (PITX2) pathway mediates transforming growth factor beta (TGFbeta) signaling to regulate cell proliferation in palatal mesenchyme during mouse palatogenesis. J Biol Chem. 2012b; 287:2353–63. [PubMed: 22123828]

Jiang W, Mitra R, Lin CC, Wang Q, Cheng F, Zhao Z. Systematic dissection of dysregulated transcription factor-miRNA feed-forward loops across tumor types. Brief Bioinform. 2016; 17:996–1008. [PubMed: 26655252]

John B, Enright AJ, Aravin A, Tuschl T, Sander C, Marks DS. Human MicroRNA targets. PLoS Biol. 2004; 2:e363. [PubMed: 15502875]

Kanehisa M. The KEGG database. Novartis Found Symp. 2002; 247:91–101. discussion 101-3, 119-28, 244-52. [PubMed: 12539951]

Kertesz M, Iovino N, Unnerstall U, Gaul U, Segal E. The role of site accessibility in microRNA target recognition. Nat Genet. 2007; 39:1278–84. [PubMed: 17893677]

Keyte A, Hutson MR. The neural crest in cardiac congenital anomalies. Differentiation. 2012; 84:25–40. [PubMed: 22595346]

Khera KS. Maternal toxicity of drugs and metabolic disorders--a possible etiologic factor in the intrauterine death and congenital malformation: a critique on human data. Crit Rev Toxicol. 1987; 17:345–75. [PubMed: 3308323]

Lan Y, Xu J, Jiang R. Cellular and Molecular Mechanisms of Palatogenesis. Curr Top Dev Biol. 2015; 115:59–84. [PubMed: 26589921]

Leslie EJ, Marazita ML. Genetics of cleft lip and cleft palate. Am J Med Genet C Semin Med Genet. 2013

Lewis BP, Burge CB, Bartel DP. Conserved seed pairing, often flanked by adenosines, indicates that thousands of human genes are microRNA targets. Cell. 2005; 120:15–20. [PubMed: 15652477]

Lomax J. Get ready to GO! A biologist's guide to the Gene Ontology. Brief Bioinform. 2005; 6:298–304. [PubMed: 16212777]

Murray JC. Gene/environment causes of cleft lip and/or palate. Clin Genet. 2002; 61:248–56. [PubMed: 12030886]

Sangani D, Suzuki A, VonVille H, Hixson JE, Iwata J. Gene Mutations Associated with Temporomandibular Joint Disorders: A Systematic Review. OAlib. 2015; 2

Schoen C, Aschrafi A, Thonissen M, Poelmans G, Von den Hoff JW, Carels CEL. MicroRNAs in Palatogenesis and Cleft Palate. Front Physiol. 2017a; 8:165. [PubMed: 28420997]

Schoen C, Glennon JC, Abghari S, Bloemen M, Aschrafi A, Carels CEL, Von den Hoff JW. Differential microRNA expression in cultured palatal fibroblasts from infants with cleft palate and controls. Eur J Orthod. 2017b

Seelan RS, Mukhopadhyay P, Pisano MM, Greene RM. Developmental epigenetics of the murine secondary palate. ILAR J. 2012; 53:240–52. [PubMed: 23744964]

Seto-Salvia N, Stanier P. Genetics of cleft lip and/or cleft palate: association with other common anomalies. Eur J Med Genet. 2014; 57:381–93. [PubMed: 24768816]

Spielman RS, McGinnis RE, Ewens WJ. Transmission test for linkage disequilibrium: the insulin gene region and insulin-dependent diabetes mellitus (IDDM). Am J Hum Genet. 1993; 52:506–16. [PubMed: 8447318]

Stanier P, Moore GE. Genetics of cleft lip and palate: syndromic genes contribute to the incidence of non-syndromic clefts. Hum Mol Genet. 2004; 13(Spec No 1):R73–81. [PubMed: 14722155]

Sun J, Gong X, Purow B, Zhao Z. Uncovering MicroRNA and Transcription Factor Mediated Regulatory Networks in Glioblastoma. PLoS Comput Biol. 2012; 8:e1002488. [PubMed: 22829753]

Sun J, Kuo PH, Riley BP, Kendler KS, Zhao Z. Candidate genes for schizophrenia: a survey of association studies and gene ranking. Am J Med Genet B Neuropsychiatr Genet. 2008; 147B: 1173–81. [PubMed: 18361404]

Suzuki A, Abdallah N, Gajera M, Jun G, Jia P, Zhao Z, Iwata J. Mouse cleft palate and its genetic implications. Data in Brief. submitted.

Suzuki A, Sangani DR, Ansari A, Iwata J. Molecular mechanisms of midfacial developmental defects. Dev Dyn. 2016; 245:276–93. [PubMed: 26562615]

Wang J, Bai Y, Li H, Greene SB, Klysik E, Yu W, Schwartz RJ, Williams TJ, Martin JF. MicroRNA-17-92, a direct Ap-2alpha transcriptional target, modulates T-box factor activity in orofacial clefting. PLoS Genet. 2013a; 9:e1003785. [PubMed: 24068957]

Wang Q, Jia P, Cuenco KT, Feingold E, Marazita ML, Wang L, Zhao Z. Multi-dimensional prioritization of dental caries candidate genes and its enriched dense network modules. PLoS One. 2013b; 8:e76666. [PubMed: 24146904]

Wang S, Sun C, Meng Y, Zhang B, Wang X, Su Y, Shi L, Zhao E. A pilot study: Screening target miRNAs in tissue of nonsyndromic cleft lip with or without cleft palate. Exp Ther Med. 2017; 13:2570–2576. [PubMed: 28565881]

Zhang B, Kirov S, Snoddy J. WebGestalt: an integrated system for exploring gene sets in various biological contexts. Nucleic Acids Res. 2005; 33:W741–8. [PubMed: 15980575]

Abbreviations

CP	cleft palate
GO	Gene Ontology
KEGG	Kyoto Encyclopedia of Genes and Genomes
miRNA	microRNA

Highlights

- 195 mouse strains with single-gene mutations and 140 mouse strains with compound-gene mutations were reported to have cleft palate.
- The genes associated with cleft palate were enriched in a category of cellular metabolism.
- A total of 18 microRNAs were involved in the regulation of multiple cleft palate genes.
- Human genotype-phenotype analysis revealed that variants in five human cleft palate genes (*IRF6, FOXE1, VAX1, WNT9B*, and *GAD1*) significantly contributed to the human cleft palate phenotype.

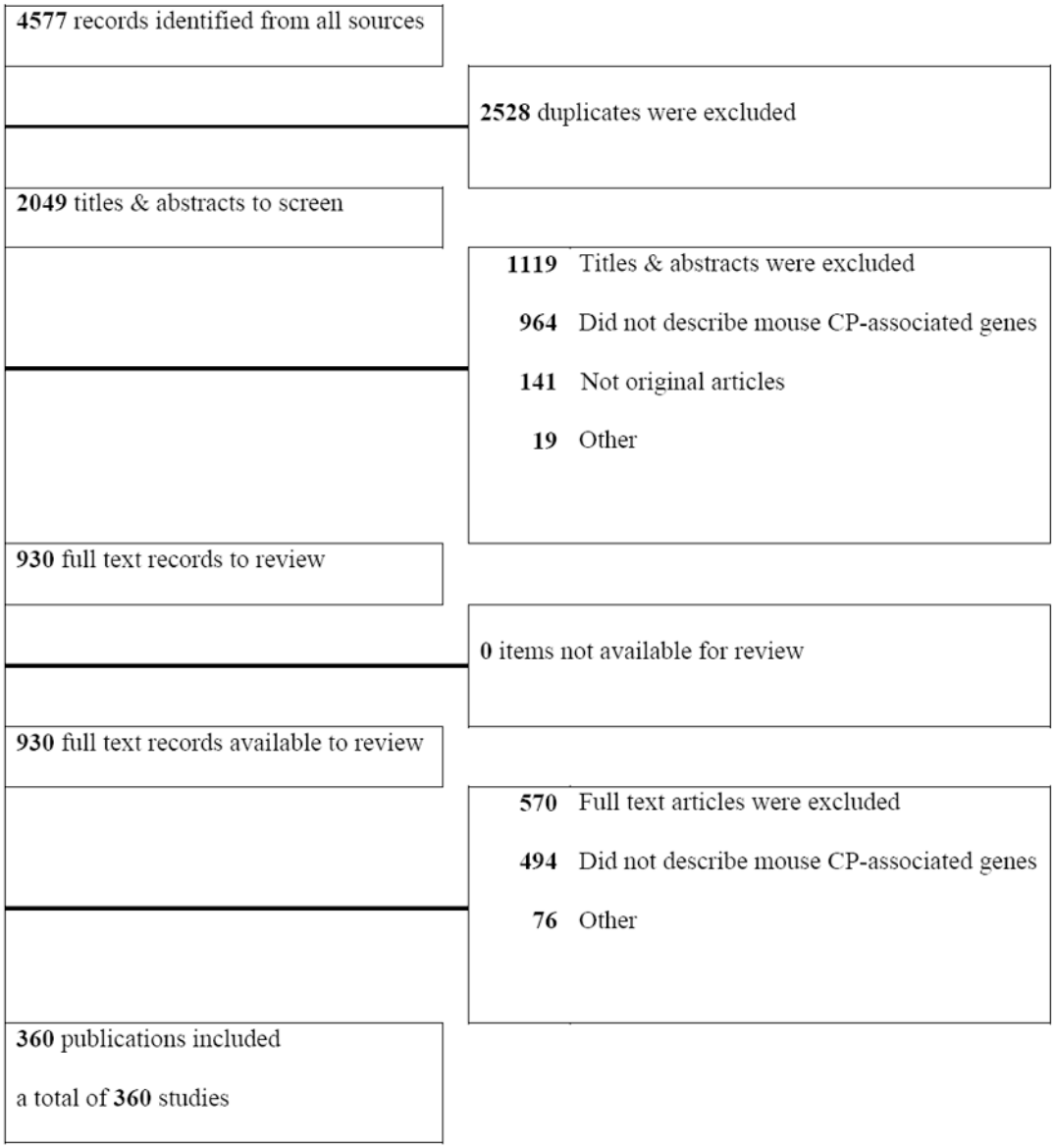

Figure 1.
PRISMA flowchart for the identification of cleft palate studies in mice

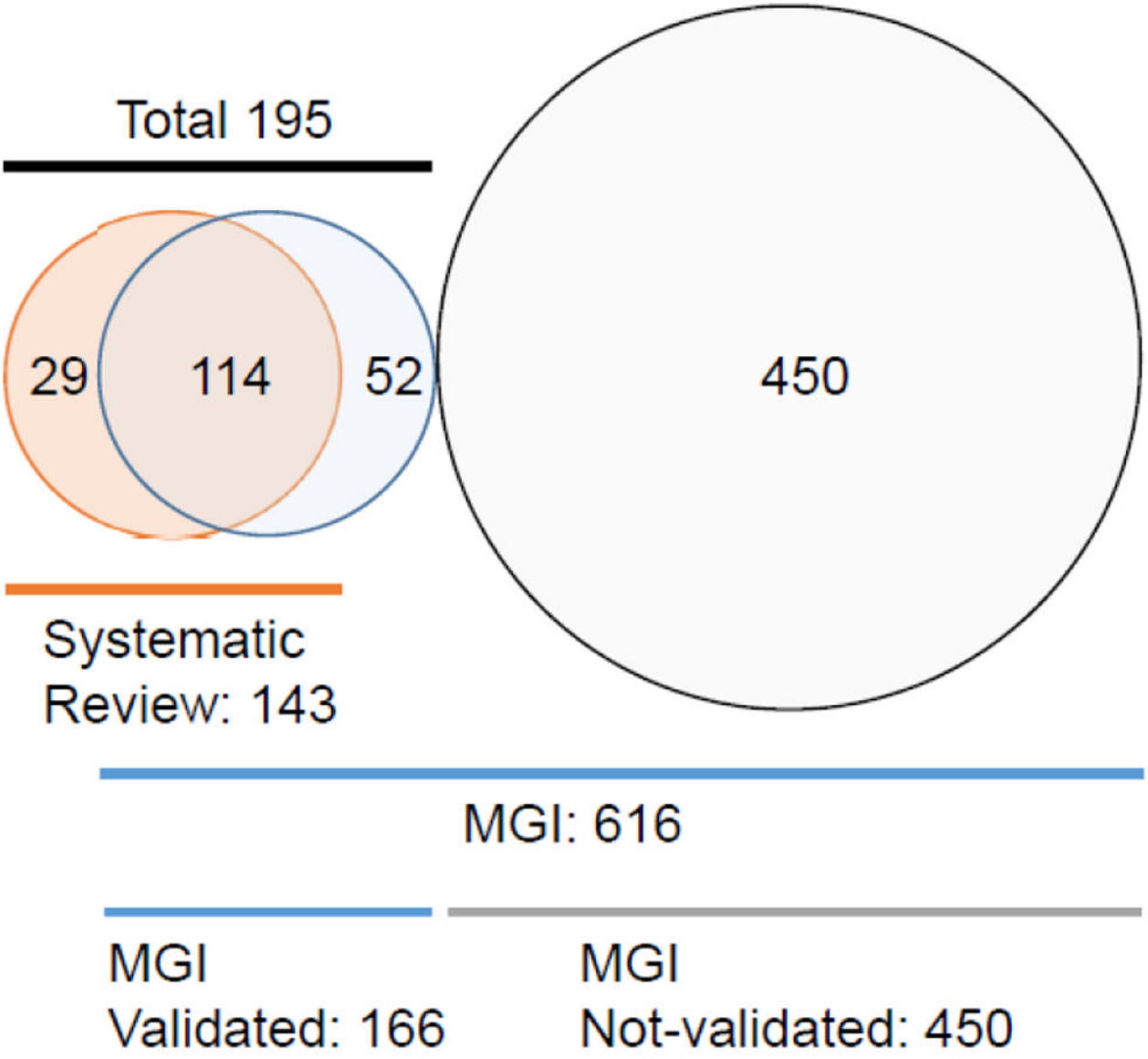

Figure 2.
Overview Diagram of CP Study

Table 1

Mice with cleft palate (CP) caused by single-gene mutations

CP type (# of strains)	Gene symbols
Complete CP (170 strains)	*Acvr1 Acvr2a Adamts20 Ap2b1 Bmp4 Bmp7 Bmpr1a Bnc2 Cacna1s Cask Cdc42 Cdkn1c Chd7 Chrd Chuk Col2a1 Col11a1 Crk Ctgf Ctnnb1 Ctnnbip1 Cyp26b1 Dhcr7 Dicer1 Dlg1 Dlx1 Dlx2 Dlx5 Dnmt3b Dph1 Edn1 Ednra Ednrb Efna5 Efnb1 Egfr Esrp1 Eya1 Fbxo11 Fbxw7 Fgf8 Fgf9 Fgf10 Fgf18 Fgfr1 Fgfr2 Fign Flna Folr1 Foxc2 Foxd3 Foxe1 Foxf2 Fst Fuz Fzd2 Gab1 Gas1 Gabrb3 Gad1 Glce Glg1 Gli2 Gli3 Grb2 Grhl3 Gsk3b Hand1 Hand2 Hdac3 Hoxa2 Hs2st1 Hspg2 Ick Ift88 Ift140 Igf2 Ilk Impad1 Inhba Inpp5e Irf6 Itga5 Itgav Itgb1 Itgb8 Jag2 Jmjd6 Kat6a Kcnj2 Kcnj13 Kdf1 Kif3a Ldb1 Lhx8 Loxl3 Lrp6 Luzp1 Map3k7 Mapk1 Men1 Meox2 Mn1 Mnt Msx1 Msx2 Nog Nosip Nrp1 Nsd2 Oca2 Ofd1 Osr2 Pak1ip1 Pax9 Pdgfc Pdgfra Pds5a Pds5b Phc1 Piga Pitx1 Pitx2 Pkdcc Prdm16 Prickle1 Prrx1 Ptch1 Ptpn11 Rac1 Rad23b Rax Recql4 Ror2 Rspo2 Runx1 Ryk Satb2 Sc5d Sfn Shh Ski Slc12a5 Slc32a1 Smo Smoc1 Snai2 Sos1 Sox2 Sox5 Sox9 Sp8 Spry2 Sumo1 Tbx2 Tcof1 Tfap2a Tgfb2 Tgfbr1 Tgfbr2 Tgfbr3 Trp53 Trp63 Twist1 Vax1 Vegfa Wls Wnt5a Wnt9b Zeb1*
Partial CP: Anterior (11 strains)	*Fgfr2 Gsc Ihh Lims1 Shox2 Sox11 Tbx1 Tbx3 Tgfb3 Tgfbr1 Tgfbr2*
Partial CP: Posterior (9 strains)	*Bnc2 Foxf2 Hic1 Mef2c Pax3 Sim2 Tgfbr1 Tgfbr2 Tshz1*
Submucous CP (16 strains)	*Acvr1 Apaf1 Arid5b Csrnp1 Eya4 Krt5 Schip1 Sgpl1 Smad4 Tbx22 Tgfb3 Tgfbr1 Tgfbr2 Tiparp Zfp640 Zfp950*

Genes involved in multiple CP types are underlined.

Table 2

Characteristics of cleft palate-associated genes

Mutation type (# of strains)	Gene symbols
Homozygous mutation: **Low penetrance (< 50%) (36 strains)**	*Adamts20 Ap2b1 Cdkn1c Ctnnbip1 Dhcr7 Dlx1 Dnmt3b Efna5 Egfr Fbxw7 Fgf9 Fign Fst Fzd2 Gab1 Glg1 Grhl3 Hs2st1 Inhba Itgb1 Jmjd6 Luzp1 Meox2 Mnt Oca2 Pds5a Prdm16 Ptch1 Ptpn11 Schip1 Ski Snai2 Sumo1 Tgfb2 Twist1 Zfp640*
Heterozygous mutation (14 strains)	*Chrd Col2a1 Fgfr2 Flna Kat6a Meox2 Mn1 Ofd1 Pds5a Prdm16 Sox9 Sumo1 Tcof1 Twist1*

Table 3

Top association SNPs and genes in candidate genes from the GWAS dataset

Top marker	Type	Gene	*P*-value
rs2235371	Missense	*IRF6*	2.96×10^{-8}
rs342308	Intron	*PDGFC*	1.51×10^{-4}
rs6585429	Intron	*VAX1*	1.67×10^{-4}

Table 4

MicroRNAs enriched for mouse cleft palate-associated genes (FDR <0.001)

miRNA family ID	miRNA	Gene symbols	FDR
miR-154	mmu-miR-381-3p	*Pbx1, Esrp1, Wnt5a, Pdgfc, Ick, Spry1, Gad1, Acvr1, Fgfr2, Tgfb3, Fbxo11, Sox6, Meox2, Gas1, Pds5b, Smoc1, Ptpn11, Six4, Twist1, Bmpr1a, Gli3, Lhx8, Acvr2a, Tiparp, Gsk3b, Lrp6, Insig1, Cdc42, Jag2, Foxf2, Mapk1, Efnb1, Nrp1, Msx2, Crk, Grhl3, Smo, Col11a1, Vegfa*	1.40×10^{-7}
miR-27	mmu-miR-27a-3p	*Csrnp1, Egfr, Runx1, Pdgfra, Spry1, Acvr1, Tgfbr1, Pax9, Eya4, Mef2c, Bmi1, Ednra, Itga5, Sos1, Gsk3b, Gab1, Eya1, Pds5b, Mmp16, Lhx8, Bmp2, Hic1, Zeb1, Acvr2a, Six1, Cdc42, Cask, Sumo1, Apaf1, Dicer1, Sox11, Gabrb3, Chd7, Tgfbr3, Pax3, Fzd7, Satb2, Ephb2, Prdm16, Spry2, Bmpr1a, Fbxw7*	3.31×10^{-5}
miR-124	mmu-miR-124-3p	*Esrp1, Ednrb, Sgpl1, Spry1, Chuk, Adamts9, Grb2, Dlx5, Itgb1, Eya4, Axin1, Kif3a, Insig2, Sos1, Meox2, Gas1, Eya1, Arid5b, Glce, Ptpn11, Six4, Mmp16, Nrp1, Vcan, Bmpr1a, Gli3, Hic1, Prrx1, Zeb1, Gsk3b, Chrd, Lrp6, Lims1, Snai2, Tm7sf2, Efnb1, Sox9, Ror2, Alx1, Dlx2, Tshz1, Tgfbr3, Pax3, Ift88, Cask, Tgfbr1, Ski, Cdc42, Dnmt3b, Fign, Fst, Pbx3, Pkdcc, Sp8, Rac1*	4.98×10^{-5}
miR-27	mmu-miR-27b-3p	*Csrnp1, Egfr, Runx1, Pdgfra, Spry1, Acvr1, Tgfbr1, Pax9, Eya4, Mef2c, Bmi1, Ednra, Itga5, Sos1, Gsk3b, Gab1, Eya1, Pds5b, Mmp16, Lhx8, Bmp2, Hic1, Zeb1, Acvr2a, Six1, Cdc42, Cask, Sumo1, Apaf1, Dicer1, Sox11, Gabrb3, Chd7, Tgfbr3, Pax3, Fzd7, Satb2, Prdm16, Ephb2, Spry2, Smad4*	4.98×10^{-5}
miR-8	mmu-miR-200a-3p	*Esrp1, Lhx6, Egfr, Map3k7, Tgfbr1, Fst, Grb2, Dlx5, Kif3a, Pitx2, Piga, Runx1, Schip1, Gab1, Zeb2, Pds5b, Prickle1, Hs2st1, Lbr, Vcan, Lhx8, Sim2, Zeb1, Acvr2a, Six1, Gli2, Cyp26b1, Tgfbr2, Mapk1, Foxc2, Rad23b, Igf2, Tgfb2, Kcnj2, Sox11, Nrp1*	6.80×10^{-5}
miR-320	mmu-miR-320-3p	*Pbx1, Vcan, Tbx2, Runx1, Dlg1, Tgfbr1, Grb2, Eya4, Cdkn1c, Bmi1, Fbxo11, Itga5, Arid5b, Ryk, Zeb2, Mn1, Pbx3, Mmp16, Bmpr1a, Hic1, Phc1, Tiparp, Insig1, Crk, Rac1, Mapk1, Wls, Ctnnb1, Fzd7, Satb2*	7.57×10^{-5}
miR-8	mmu-miR-141-3p	*Esrp1, Lhx6, Egfr, Map3k7, Tgfbr1, Fst, Grb2, Dlx5, Kif3a, Pitx2, Piga, Schip1, Gab1, Zeb2, Pds5b, Prickle1, Hs2st1, Lbr, Vcan, Lhx8, Sim2, Zeb1, Acvr2a, Six1, Gli2, Cyp26b1, Tgfbr2, Mapk1, Foxc2, Rad23b, Igf2, Tgfb2, Kcnj2, Sox11, Runx1*	1.35×10^{-4}
miR-203	mmu-miR-203-3p	*Dlg1, Dnmt3b, Ick, Pdgfra, Fign, Dlx5, Eya4, Mef2c, Pitx2, Hand2, Ap2b1, Bmi1, Fbxo11, Vegfa, Eya1, Glce, Pbx3, Mmp16, Vcan, Gli3, Bmp2, Edn1, Slc32a1, Acvr2a, Insig1, Cask, Snai2, Gad2, Shh, Gabrb3, Nrp1, Igf2r, Wls, Crk, Grhl3, Tshz1, Ski, Trp63, Bnc2*	1.35×10^{-4}
miR-21	mmu-miR-21a-5p	*Tbx2, Sox2, Trim33, Sox5, Spry1, Gad1, Rspo2, Mef2c, Pitx2, Fbxo11, Plekha1, Alx1, Sox6, Msx1, Ski, Chd7, Spry2, Tgfbr2, Tgfbr3*	1.48×10^{-4}
miR-30	mmu-miR-30a-5p	*Pax3, Ednrb, Runx1, Adamts9, Mdm4, Acvr1, Fst, Fign, Eya4, Snai1, Kif3a, Piga, Insig2, Mnt, Ednra, Arid5b, Sos1, Pds5b, Glce, Prickle1, Fgf10, Six4, Ephb2, Lhx8, Pbx2, Six1, Gli2, Apaf1, Jag2, Sox9, Nrp1, Tbx22, Igf2r, Crk, Hoxa2, Rad23b, Fzd7, Chd7, Satb2, Fzd2, Egfr, Mdm2, Inhba*	2.05×10^{-4}
miR-25	mmu-miR-25-3p	*Ick, Fst, Tbx3, Pkdcc, Pax9, Hand2, Hand1, Cdkn1c, Itga5, Zeb2, Pds5b, Glce, Luzp1, Twist1, Mmp16, Plekha1, Slc32a1, Sim2, Insig1, Cask, Sox11, Tcf21, Slc12a5, Itgav, Col11a1, Satb2, Ski, Fbxw7*	4.95×10^{-4}
miR-329	mmu-miR-543-3p	*Pbx1, Fgfr2, Rspo2, Tgfbr1, Fign, Itgb1, Eya4, Cask, Hand2, Dlx1, Sos1, Schip1, Eya1, Pds5b, Hs2st1, Vcan, Twist1, Bmp2, Acvr2a, Dicer1, Mapk1, Ror2, Mmp14, Sox6, Itgb8, Fzd7, Efna5, Six4*	4.95×10^{-4}
miR-590	mmu-miR-590-5p	*Tbx2, Sox2, Trim33, Sox5, Spry1, Gad1, Rspo2, Pitx2, Fbxo11, Plekha1, Alx1, Sox6, Ski, Chd7*	4.95×10^{-4}
miR-25	mmu-miR-92a-3p	*Ick, Fst, Tbx3, Pkdcc, Pax9, Hand2, Hand1, Cdkn1c, Itga5, Zeb2, Pds5b, Luzp1, Twist1, Mmp16, Plekha1, Slc32a1, Sim2, Insig1, Cask, Sox11, Tcf21, Slc12a5, Itgav, Col11a1, Satb2, Ski, Shox2, Trp63*	4.95×10^{-4}
miR-154	mmu-miR-377-3p	*Ednrb, Wnt5a, Map3k7, Chuk, Adamts9, Fign, Pax9, Eya4, Axin1, Pitx2, Hand2, Smad4, Vegfa, Gsk3b, Meox2, Zeb2, Pds5b, Prdm16, Phc2, Hs2st1, Pdgfra, Six4, Shox2, Acvr2a, Gad2, Shh, Crk, Ephb3, Insig2, Pax3, Sfn*	5.78×10^{-4}
NA	mmu-miR-882	*Rspo2, Fst, Fign, Vegfa, Ptprf, Hs2st1, Ephb2, Pbx2, Gsk3b, Cdc42, Efnb1, Igf2r, Pbx1, Slc12a5, Tshz1, Fgf10, Prrx1*	5.78×10^{-4}

miRNA family ID	miRNA	Gene symbols	FDR
miR-185	mmu-miR-185-5p	*Rspo2, Fst, Fign, Grb2, Vegfa, Ptprf, Hs2st1, Ephb2, Pbx2, Gsk3b, Cdc42, Efnb1, Igf2r, Pbx1, Plekha1, Slc12a5, Tshz1, Ctnnb1, Vcan, Fgf10, Prrx1*	7.95×10^{-4}
miR-29	mmu-miR-29b-3p	*Ctnnbip1, Pdgfc, Dnmt3b, Spry1, Adamts9, Fign, Itgb1, Efna5, Col2a1, Pdgfrb, Vegfa, Gsk3b, Plekha1, Schip1, Ephb3, Gab1, Ptpn11, Bmpr1a, Phc1, Insig1, Dicer1, Cdc42, Lims1, Adamts20, Ctnnb1, Tgfb2, Col11a1, Acvr2a, Luzp1, Ski, Sox2, Tgfb3*	7.95×10^{-4}

FDR: false discovery rate, which was obtained by Benjamini–Hochberg adjustment for multiple test correction (Benjamini and Hochberg, 1995) of the *p* value in Fisher's exact test.